Low-Density Parity Check code based Multi-band OFDM for UWB Communications
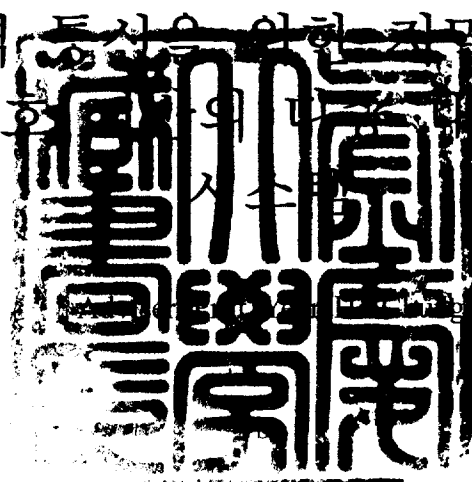
초광대역 통신을 위한 저밀도 패리티 검사 부호 기반의 다중대역 OFDM

Mi Ra Ryu

A thesis submitted in partial fulfillment of the requirements

for the degree of

Master of Engineering

in the Department of Telematics Engineering, The Graduate School,

Pukyong National University

February 2006

류미라의 공학석사 학위논문을 인준함.

2005년 12월 22일

주　　심　공학박사　정 신 일
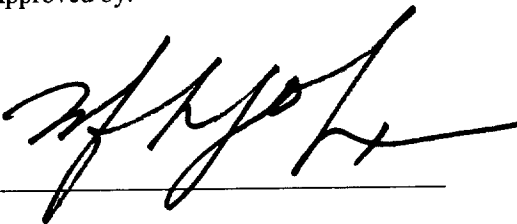
위　　원　공학박사　박 규 칠

위　　원　공학박사　정 연 호

Low-Density Parity Check Code based

Multi-band OFDM for UWB Communications
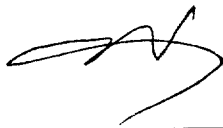
A dissertation

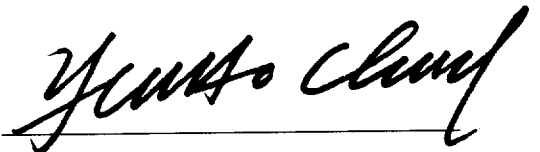**by**

Mi Ra Ryu

Approved by:

_____

(Chairman)   Prof. Shin Il JEONG

_____

(Member)   Prof. Kyu Chil PARK

_____

(Member)   Prof. Yeon Ho CHUNG

December 22, 2005

CONTENTS

LIST OF FIGURES

LIST OF TABLES

초광대역 통신을 위한 저밀도 패리티 검사 부호 기반의

다중 대역 OFDM 시스템

류 미 라

부경대학교 대학원 정보통신공학과

요 약

근거리에서 무선 고속 정보 전송을 위한 기술로서 초광대역(UWB: Ultra Wideband) 무선기술 시스템이 주목 받고 있다. UWB 구현을 위한 기술로서 다중 대역 OFDM(MB-OFDM: Multi-Band Orthogonal Frequency Division Multiplexing) 시스템을 적용하는데 스펙트럼을 다중 대역으로 나눔으로써 고속 데이터 전송을 한다. 본 논문에서는 친 사용자 시뮬레이션 환경을 제공하는 SPW(Signal Processing Worksystem) 시뮬레이션 플랫폼을 이용하여 IEEE802.15.3a 에서 제안된 다중 대역 OFDM 시스템과 LDPC(Low-Density Parity Check) 코드를 적용한 시스템을 구현하여 성능을 비교, 분석하였다. 시뮬레이션 결과에 의하면 제안하는 LDPC 기반의 다중 대역 OFDM 시스템에서 향상된 비트 오율을 얻을 수 있었다.

Low-Density Parity Check codes based Multi-band OFDM

for UWB Communications

Mi Ra Ryu

Department of Telematics Engineering,

Graduate School, Pukyong National University

Abstract

Ultra Wideband (UWB) technology is a promising solution to very high speed data transmission at short ranges Multi-band Orthogonal Frequency Multiplexing (MB-OFDM) is employed to transmit high speed data in ultra wideband spectrum by dividing the available spectrum into multiple bands. In multicarrier transmission schemes, a powerful error correcting code is applied to enhance the performance. In this thesis, a Low-Density Parity Check (LDPC) code based MB-OFDM system is proposed. The MB-OFDM system considered in the study is in full conformance with the IEEE 802.15.3a standard. Performance comparison shows that the proposed LDPC-based MB-OFDM provides a significant performance gain over the IEEE 802.15.3a standard

Ⅰ. Introduction

In the future wireless communication systems high speed data transmission is essential with high quality. Recently, Ultra Wideband (UWB) transmission technology has been considered as a promising solution to high speed transmission. This technology delivers data at a rate of 110 Mbps in realistic multipath Multi-band OFDM (MB-OFDM) for high bit rate Wireless Personal Area Netwoks (WPANs) [1]. The IEEE 802.15.3a for WPANs is based on OFDM and can deliver data at a rate of up to 480 Mbps. In this system, the whole available ultra wideband spectrum between 3.1-10.6 GHz is divided into a total of 122 sub-bands that are modulated using quadrature phase shift keying (QPSK) [2]. The bandwidth of each sub-band is larger than 500 MHz in compliance with the FCC rules for UWB transmission. In MB-OFDM, data are transmitted using parallel narrowband sub-channels and inter symbol interference (ISI) can be eliminated by adding cyclic prefix [3]. The IEEE 802.15.3a system supports multiple modes of operations, i.e. 3-band (mandatory) and 7-band (optional) modes. In multipath environments, some of the sub-carriers suffer from a deep fade, causing the overall bit error rate to be dependent on the signal-to-noise ratio (SNR) of the weakest sub-carriers, instead of the average received power [2]. For this reason, it is essential to employ an error correcting code for the overall bit error rate to be dependent upon the average received power. Recently, a powerful error correcting code of the

1

Low-Density Parity Check (LDPC) code has been proposed and its iterative decoding algorithm was invented by Gallager [4]. The LDPC codes are known to achieve the performance close to the Shannon limit with little power [5]. In this thesis, we propose an MB-OFDM system with LDPC codes implemented for UWB communications.

This thesis evaluates the performance of the Multi-Band OFDM system under various IEEE 802.15.3a channel scenarios. To perform this, we use SPW platform whose flexibility makes the systems design more effective and SPW provides an easy tool to analyze the performance.

The outline of this thesis is as follows. In Section II, we present a general background to UWB. In Section III, we discuss Low Density Parity Check Code from basic concepts and construction techniques. In Section IV, we describe the multi-band OFDM system from basic concepts to important factors. Section V provides simulation results and demonstrates the performance of the LDPC code via the multi-band OFDM system environment using SPW platform. Finally, Section VI presents conclusions.

Ⅱ. Ultra Wideband System

Historically, UWB radar systems were developed mainly as a military tool because they could "see through" trees and beneath ground surfaces. However, recently, UWB technology has been focused on consumer electronics and communications. Ideal targets for UWB systems are low power, low cost, high data rates, precise positioning capability and extremely low interference.

UWB technology is different from conventional narrowband wireless transmission technology – instead of broadcasting on separate frequencies, USB spreads signals across a very wide range of frequencies. The typical sinusoidal radio wave is replaced by trains of pulses at hundreds of millions of pulses per second. The wide bandwidth and very low power makes UWB transmission appear as background noise.

2.1 Historical notes of UWB

UWB would be regarded as a new technology in the sense that it provides the means to support high data rates, smaller and lower powered devices. However, UWB is a new engineering technology in that no new physical properties have been discovered.

The dominant method of wireless communication today is based on sinusoidal waves. Sinusoidal electromagnetic waves have become so

universal in radio communications that many people are not aware that the first communication systems were in fact pulse-based. This paradigm shift for today's engineers from sinusoids to pulses requires the most shift in focus.

In 1973 the first US patent was awarded for UWB communications. Various applications with UWB, such as automobile collision avoidance positioning systems, liquid-level sensing and altimetry were developed. Most of the applications and development occurred in the military or work funded by the US Government under classified programs. For the military, accurate radar and low probability of intercept communications were the driving forces behind research and development.

In these early days, UWB was referred to as *baseband, carrier-free* and *impulse* technology. The US Department of Defense is believed to be the first to have started to use the term *ultra wideband* [6].

In late 1990s, it has moved to commercialize UWB communication devices and systems. Companies such as Time Domain and in particular startups like XtreamSpectrum were formed around the idea of consumer communication using UWB.

2.2 Key benefits of UWB

The key benefits of UWB can be summarized as:

• high data rate

- low equipment cost

- multipath immunity

- ranging and communication at the same time

The high data rates are the most compelling aspect from a user's point of view and also from a commercial manufacturer's position. Higher data rates can enable new applications and devices that would not have been possible up until now. Speeds of over 100 Mbps have been demonstrated, and the potential for higher speeds over short distance is expected. The extremely large bandwidth occupied by UWB gives this potential.

The ability to directly modulate a pulse onto an antenna enables a simple transmitter, leading many manufacturers to get excited by the possibilities for extremely cheap transceivers. This is possible by eliminating many of the components required for conventional sinusoidal transmitters and receivers.

The narrow pulses used by UWB, which also give the extremely wide bandwidth, provide a fine resolution of reflected pulses at the receiver. This is important in wireless communication, as pulses interfering with each other are the major obstacle to error-free communication.

Finally, the use of both object location and high speed data communication in the same wireless device presents intriguing possibilities for new devices and applications. For example, simultaneous automatic collision avoidance radar and communication can give accident-free smooth traffic flow.

2.3 UWB and shannon's theory

The benefits and possibilities of UWB can be best summarized by examining Shannon's famous capacity equation. Capacity is important as more demanding audio-visual applications require higher bit rates.

Shannon's equation is expressed as

$$C = B \log\left(1 + \frac{S}{N}\right) \qquad (2.1)$$

where C is the maximum channel capacity, with units [bits/second]; B is the channel bandwidth [Hz]; S is the signal power in watts [W] and N is the noise power in watts [W] [7].

In order to improve the capacity of the channel, we can increase the bandwidth, the signal power or decrease the noise. That is, we also can see that the capacity of a channel grows linearly with increasing bandwidth B, but only logarithmically with signal power S.

The ultra wideband channel has an abundance of bandwidth and can trade off some of the bandwidth for reduced signal power and interference from other sources. Thus, from Shannon's equation we can see that UWB systems have a great potential for high-capacity in wireless communications.

The main concerns of wireless communication are:

- the distance between transmitter and receiver

- simultaneous communication for many users

- sending the data very quickly

- sending and receiving a large amount of data

The first wireless communication systems, such as wireless communication at sea, were meant to communicate between ships separated by large distances. However, the amount of data that could be effectively transferred was extremely small and communication took a long time. Only one person can "talk" using Morse code at a time. More recently, cellular telephone systems have simultaneous communication for many users. The distance between the base station and the user is limited to a few kilometers. It can be classified as a system where a moderate amount of data can be sent reasonably quickly. An ultra wideband system is focused on the latter two attributes: a large amount of data that can be transmitted very quickly. This is at the expense of distance. The precise tradeoffs are more complex and will depend on the particular application.

2.4 Challenges for UWB

While UWB has many reasons to make it an exciting and useful technology for future wireless communications, it also has some challenges to become a popular and ubiquitous technology.

The most obvious one to date has been regulatory problems. Wireless communications have been regulated to avoid interference between different users of the spectrum. Since UWB occupies wide bandwidth, there are many users whose spectrum will be affected and need to be convinced. In many cases these users have paid to have exclusive use of the spectrum.

Other challenges include the industry coming to agreed standards for inter-operability of UWB devices. At present no clear standard has emerged, and the possibility of several competing UWB standards is extremely likely.

Many technical and implementation issues remain to be determined. The promise of low-cost devices is obvious, but the added complexity to combat interference and low-power operation may bring cost increases similar to current wireless devices.

III. Low Density Parity Check (LDPC) code

In 1962, Gallager introduced a class of linear codes, known as low-density parity check (LDPC) codes, and presented iterative probabilistic decoding algorithm. Later, Tanner extended Gallager's probabilistic decoding algorithm to the more general case where the parity-checks are defined by subcodes, instead of simple single parity-check equations [8]. Earlier, it was shown that LDPC codes have a minimum distance that grows linearly with the code length and that errors up to the minimum distance could be corrected with a decoding algorithm with almost linear complexity.

It is shown that LDPC codes can get as close to the Shannon limit as turbo codes. Later, irregular LDPC codes were shown to outperform turbo codes of approximately the same length and rate, when the block length is large. The best rate 1/2 LDPC code, with a block length of 10,000,000, achieved a record 0.0045 dB away from the Shannon limit for binary transmission over an AWGN channel [5].

3.1 Construction of LDPC code

LDPC codes are defined as codes using a sparse parity check matrix with the number of 1's per column (column weight) and the number of 1's per row (row weight), both of which are very small compared to the block length. LDPC codes are classified into two groups, regular LDPC codes and

irregular LDPC codes [9]. Regular LDPC codes have a uniform column weight and row weight, and irregular LDPC codes have a nonuniform column weight. We describe an LDPC code defined $M \times N$ parity check matrix H as (N, K) LDPC, where $K = N - M$ and the code rate is $R = K / N$. In the case that the H doesn't have full rank, $K > N - M$ and the error performance of a LDPC code become worse. Thus, when we construct the parity check matrix H, we ensure that all the rows of the matrix are linearly independent. LDPC codes can be decoded by using a probability propagation algorithm known as the sum-product or belief propagation algorithm. LDPC codes have better block error performance than turbo codes, because the minimum distance of an LDPC code increases proportional to the code length with a high probability. Such a property is desirable for the high-bit-rate transmission that requires very low frame error probability.
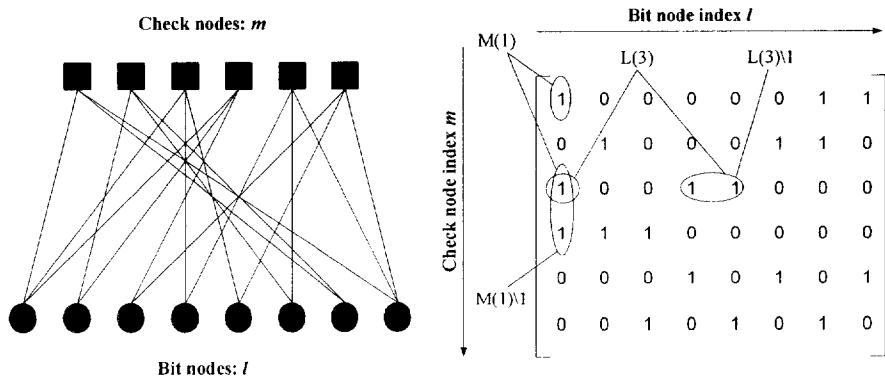
3.2 Sum-product algorithm

Figure 3.1 Factor Graph

First, we describe the notations of the sum-product algorithm in Figure 2.1. $M(l)$ denotes the set of check nodes that are connected to the bit node l, i.e., position of "1"s in the lth column of the parity check matrix. $L(m)$ denotes the set of bits that participates in the mth parity check equation, i.e., the positions of "1" in the mth row of the parity check matrix. $L(m) \setminus l$ represents the set $L(m)$ with the lth bit excluded and $M(l) \setminus m$ represents the set $M(l)$ with the mth check bit excluded. $q^i_{l \to m}$, where $i = 0, 1$ denotes the

probability information that the bit node l sends to the check m, indicating $P(x_l = i)$. $r^i_{m \to l}$ denotes the probability information that the mth check node

gathers for the lth bit being i. In other words, $r^i_{m \to l}$ is the likelihood

information for $x_l = i$ from the mth parity check equation, when the

probabilities for other bits are designated by the $q^i_{l \to m}$. There, $r^i_{m \to l}$ can be

considered as the "extrinsic" information for the lth bit node from the mth check node.

For binary codes, the sum-product algorithm can be performed more efficiently in Log domain, where the probabilities are equivalently characterized by the log-likelihood ratios (LLRs):

$$L(r_{m \to l}) \square \log \frac{r^1_{m \to l}}{r^0_{m \to l}}, L(q_{m \to l}) \square \log \frac{q^1_{m \to l}}{q^0_{m \to l}} \qquad (3.1)$$

$$L(p_l) \square \log \frac{p^1_l}{p^0_l}, L(q_l) \square \log \frac{q^1_l}{q^0_l} \qquad (3.2)$$

Note that p_l^i represents the likelihood that the lth bit is i.

Initialization

Each bit node l is assigned an a priori LLR $L(p_l)$. In the case of equiprobable inputs on a memoryless AWGN channel with BPSK,

$$L(p_l) = \log \frac{P(y_l \mid x_l = +1)}{P(y_l \mid x_l = -1)} = \frac{2}{\sigma^2} y_l \qquad (3.3)$$

where, x, y represent the transmitted bit and received bit, respectively, and σ^2 is the noise variance. For every position (m, l) such that $H_{ml} = 1$, where H_{ml} represents the element of the mth row and the lth column in the parity-check matrix H, $L(q_{l \to m})$ and $L(r_{m \to l})$ are initialized as equation (3.4) and (3.5).

$$L(q_{l \to m}) = L(p_l) \qquad (3.4)$$

$$L(r_{m \to l}) = 0 \qquad (3.5)$$

Checks to bits

Each check node m gathers all the incoming information $L(q_{l \to m})$'s, and updates the belief on the bit l based on the information from all other bits connected to the check node m.

$$L(r_{m \to l}) = 2 \tanh^{-1} \left(\prod_{l' \in L(m) \backslash l} \tanh\left(L(q_{l' \to m}) / 2 \right) \right) \qquad (3.6)$$

Bits to checks

Each bit node l propagated its probability to all the check nodes that connect to it.

$$L(q_{l \to m}) = L(p_l) + \sum_{m' \in M(l)} L(r_{m' \to l}) \qquad (3.7)$$

Checks to stop criterion

The decoder obtains the total *a posteriori* probability for the bit l by summing the information from al the check nodes that connect to the bit l.

$$L(q_l) = L(p_l) + \sum_{m \in M(l)} L(r_{m \to l}) \qquad (3.8)$$

Hard decision is made on the $L(q_l)$, and the resulting decoded input vector $\hat{x}$ is checked against the parity-check matrix H. If $H\hat{x} = 0$, the decoder stops and outputs $\hat{x}$. Otherwise, it repeats the previous steps. The sum-product algorithm sets the maximum number of iterations (max-iteration). If the number of iterations becomes the maximum number of iterations, the decoder stops and output $\hat{x}$.

Ⅳ. LDPC based Multi-band OFDM system

Multi-band Orthogonal Frequency Division Multiplexing (MB-OFDM) is a suitable solution to implement high speed data in ultra wideband spectrum by dividing the available spectrum into multiple bands. Due to the importance of error correcting codes for OFDM system, it is essential to employ a powerful error correcting code for MB-OFDM system to improve the performance.

In this thesis, we employ a LDPC code for improving the MB-OFDM performance. Prior to describing LDPC-based MB-OFDM system, an overview of a UWB system is provided together with its physical layer structure. The proposed LDPC-based MB-OFDM is then described in detail.

4.1 Overview of a UWB system

The actual RF transmitted signal is related to the complex baseband signal as equation (4.1):

$$r_{RF}(t) = \text{Re}\left\{ \sum_{k=0}^{N-1} r_k(t - kT_{SYM}) \exp(j2\pi f_k t) \right\} \qquad (4.1)$$

where $\text{Re}(\cdot)$ represents the real part of a complex variable, $r_k(t)$ is the

complex baseband signal of the kth OFDM symbol and is nonzero over the

interval from 0 to T_{SYM}, N is the number of OFDM symbols, T_{SYM} is the symbol interval, and f_k is the center frequency for the kth band.

All of the OFDM symbols $r_k(t)$ can be constructed using an inverse Fourier transform (IFFT) with a set of coefficient C_n, where the coefficients are defined as data, pilots, and training symbols:

$$r_k(t) = \begin{cases} \sum_{n=-N_{ST}/2}^{N_{ST}/2} C_n \exp(j2\pi n \Delta_f)(t - T_{CP}), & t \in [T_{CP}, T_{FFT} + T_{CP}] \\ 0 & , \quad others \end{cases} \qquad (4.2)$$

The parameter Δ_f is the subcarrier frequency spacing, N_{ST} is the number of total subcarriers used. The resulting waveform has a duration of $T_{FFT}=1/\Delta_f$. Shifting the time by T_{CP} creates the "circular prefix" which is in used in OFDM to mitigate the effects of multipath. The parameter T_{GI} is the guard interval duration.

A common way to implement the inverse Fourier transform is by an inverse Fast Fourier Transform (IFFT) algorithm. After performing the IFFT, a zero-padded prefix of length 32 is pre-appended to the IFFT output and a guard interval is added at the end of the IFFT output to generate an output with the desired length of 165 samples.

4.2 UWB Physical Layer Convergence Procedure (PLCP) sublayer

This section provides a method for converting the IEEE 802.15 PHY sublayer service data units (PSDUs) to PLCP protocol data units (PPDUs). During the transmission, the PSDU shall be provided with a PLCP preamble and header to create the PPDU. At the receiver, the PLCP preamble and header are processed to aid in the demodulation, decoding, and delivery of the PSDU.

4.2.1 PLCP frame format

Figure 4.1 shows the format for PHY frame including the PLCP preamble, PLCP header (PHY header, MAC header, header check sequence, tail bits, and pad bits), MAC frame body (frame payload plus frame check sequence), tail bits, and pad bits.
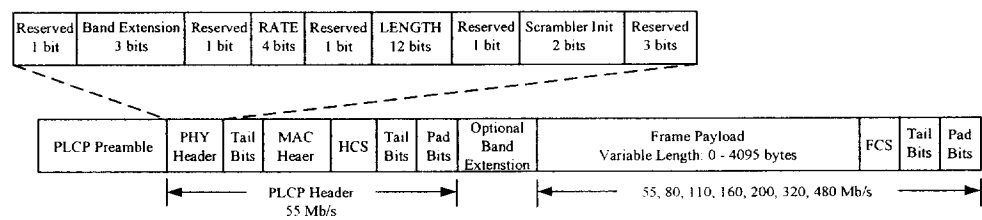

Figure 4.1 PLCP frame format for a Mode 1 device

The PHY sublayer pre-appends the PHY header plus the tail bits to the MAC header and then calculates the header check sequence (HCS) and tail bits. The tail bits are added after the PHY header to return to the "zero state". Pad bits are added after the tail bits in order to align the data stream on an

OFDM symbol boundary. Tail bits are also added to the MAC frame body. If the size of the MAC frame body plus tail bits are not an integer multiple of the bits/OFDM symbol, then pad bits are added to the end of the tail bits in order to align the data stream on the OFDM symbol boundaries.

The PLCP preamble is sent first, followed by the PLCP header, an optional band extension sequence, the frame payload, the frame check sequence (FCS), the tail bits, and the pad bits. The PLCP header, MAC header, HCS, and tail bits shall be modulated using an information data rate of 55 Mbps. The PLCP header is always transmitted using Mode 1. The remainder of the PLCP frame (frame payload, FCS, tail bits, and pad bits) is sent at the desired information data rate of 55, 80, 160, 200, 320, or 480 Mbps using either Mode 1 or Mode 2. The data rate dependent modulation parameters are listed in Table 4.1.

Table 4.1 Rate-dependent parameters

Data rate (Mbps)	Modulation	Coding Rate (R)	Conjugate Symmetric Input to IFFT	Time Spreading	Overall Spreading gain	Coded bits per OFDM Symbol
55	QPSK	11/32	YES	YES	4	100
80	QPSK	1/2	YES	YES	4	100
110	QPSK	11/32	NO	YES	2	200
160	QPSK	1/2	NO	YES	2	200
200	QPSK	5/8	NO	YES	2	200
320	QPSK	1/2	NO	NO	1	200
480	QPSK	3/4	NO	NO	1	200

A list of the timing parameters associated with the OFDM PHY is listed in Table 4.2.

Table 4.2 Timing-related parameters

Parameters	Value
N_{SD}: Number of data subcarriers	100
N_{SDP}: Number of defined pilot carriers	12
N_{SG}: Number of total subcarrier used	10
N_{ST}: Number of total subcarriers used	122(=N_{SD}+N_{SDP}+N_{SG})
Δ_F: Subcarrier frequency spacing	4.125 MHz(=528 MHz/128)
T_{FFT}: IFFT/FFT period	242.42 ns (=32/528 MHz)
T_{CP}: Cyclic prefix duration	60.61 ns (=32/528 MHz)
T_{GI}: Guard interval duration	9.47 ns (=5/528 MHz)
T_{SYM}: Symbol interval	312.5 ns (T_{CP}+T_{FFT}+T_{GI})

If we consider the Mode 1 of MB-OFDM system, it consists only three bands. Figure 4.2 illustrates how the OFDM symbols are transmitted in a MB-OFDM system. In this example, it has been implicitly assumed that the time-frequency coding (TFC) is performed across just three OFDM symbols.

Guard Interval for TX/RX
Switching Time

9.5 ns

3168

60.6 ns   Cyclic
Prefix

3696

312.5 ns

4224

4752

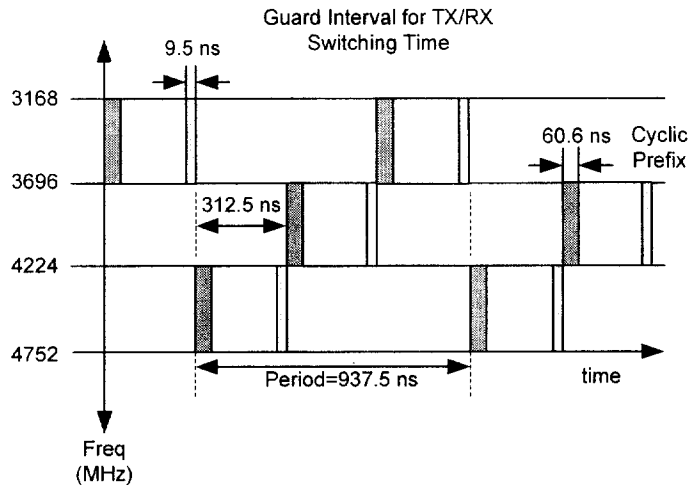Period=937.5 ns   time

Freq
(MHz)

Figure 4.2 Example of TF coding for an MB-OFDM system

In a MB-OFDM system, a guard interval (9.5 nsec) is appended to each OFDM symbol and a zero-padded prefix (60.5 nsec) is inserted at the beginning of each OFDM symbol. The guard interval ensures that there is sufficient time for the transmitter and receiver to switch to the next carrier frequency. A zero-padded prefix provides both robustness against multi-path and eliminates the need for power back-off at the transmitter.

4.2.2 PLCP preamble

A standard PLCP preamble shall be added prior to the PLCP header to aid receiver algorithms related to synchronization, carrier-offset recovery, and channel estimation. The standard PLCP preamble, which is shown in Figure 4.3, consists of three distinct portions: packet synchronization sequence, frame synchronization sequence, and the channel estimation sequence. The packet synchronization sequence shall be constructed by

appending 21 periods, denoted as $\{PS_0, PS_1, \ldots, PS_{20}\}$, of a time domain sequence. Each piconet will use a distinct time-domain sequence. These time-domain sequences are defined in [2]. Each period of the timing synchronization sequence shall be constructed by pre-appending 32 "zero samples" and by appending a guard interval of 5 "zero samples" to the sequences. This portion of the preamble can be used for packet detection and acquisition, coarse carrier frequency estimation, and symbol timing.

The frame synchronization sequence will be constructed by appending 3 periods, denoted as $\{FS_0, FS_1, FS_2\}$, of a 180 degree rotated version of the time-domain sequence specified in [2]. Each period of the frame synchronization sequence shall be constructed by pre-appending 32 "zero sample" and by appending a guard interval of 5 "zero samples" to the sequences defined in [2]. This portion of the preamble can be used to synchronize the receiver algorithm within the preamble.

Finally, the channel estimation sequence shall be constructed by appending 6 periods, denoted as $\{CE_0, CE_1, \ldots, CE_5\}$, of the OFDM training symbol. This training symbol is generated by passing the frequency-domain sequence, defined in [2], though the IFFT, and pre-appending the output with 32 "zero samples" and appending and a guard interval consisting of 5 "zero samples" to the resulting time-domain output. This portion of the preamble can be used to estimate the channel frequency response, for fine carrier frequency estimation, and fine symbol timing.
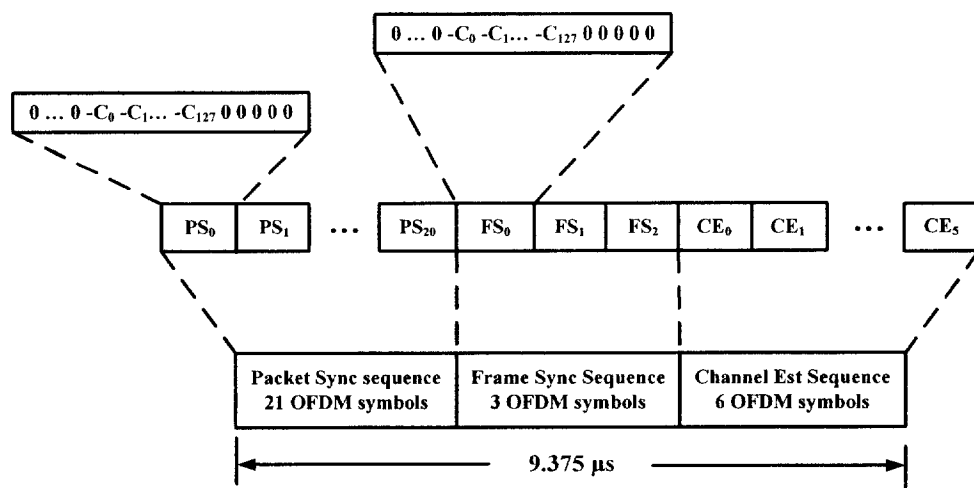
$$0 \ldots 0 -C_0 -C_1 \ldots -C_{127}\ 0\ 0\ 0\ 0$$

$$0 \ldots 0 -C_0 -C_1 \ldots -C_{127}\ 0\ 0\ 0\ 0$$

| PS_0 | PS_1 | $\cdots$ | PS_{20} | FS_0 | FS_1 | FS_2 | CE_0 | CE_1 | $\cdots$ | CE_5 |

| Packet Sync sequence 21 OFDM symbols | Frame Sync Sequence 3 OFDM symbols | Channel Est Sequence 6 OFDM symbols |

9.375 μs

Figure 4.3 Standard PLCP preamble format

4.2.3 PLCP Header

The OFDM training symbols followed by the PHY header, which contains the BAND EXTENSION field, the RATE of the MAC frame body, the length of the frame payload, and the seed identifier for the data scrambler. The BAND EXTENSION field specifies the mode of transmission for the frame payload. The RATE field conveys the information about the type of modulation, the coding rate, and the spreading factor used to transmit the MAC frame body.

The PLCP header field shall be composed of 28 bits. Bits 1 to 3 shall encode the BAND EXTENSION field. Bit 4 shall be reserved for future use. Bits 5 to 8 shall encode the RATE field. Bit 9 shall be reserved for future use. Bits 10 to 21 shall encode the LENGTH field, with the least significant

21

bit (LSB) being transmitted first. Bit 22 shall be reserved for future use. Bits 23 and 24 shall encode the initial state of the scrambler, which is used to synchronize the descrambler of the receiver. Bits 25 to 27 shall be reserved for future use.
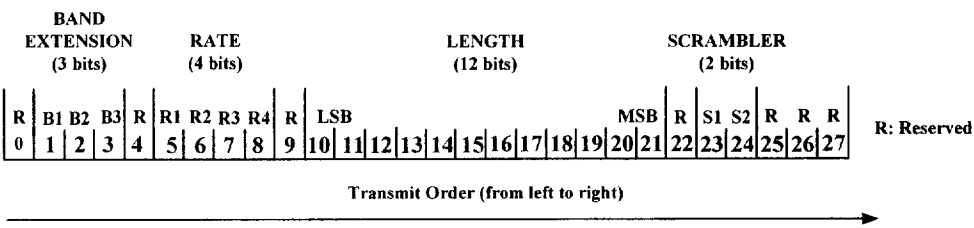

Figure 4.4 PLCP Header bit assignment

4.2.4 Data scrambler

A scrambler shall be used for the MAC header, HCS, and MAC frame body. The PLCP preamble, PLCP header, and tail bits shall not be scrambled.

4.2.5 Bit interleaving

The coded bit stream is interleaved prior to modulation. Bit interleaving provides robustness against burst errors. It is performed in two stages: symbol interleaving and tone interleaving. The symbol interleaver permutes the bit across OFDM symbols to exploit frequency diversity across the sub-bands, while the tone interleaver permutes the bits across the data tones within an OFDM symbol to exploit frequency diversity across

tones and provide robustness against narrow-band interferes.

4.3 General requirements

4.3.1 Operating band frequencies

In February 2002, the FCC allocated 7.5 GHz of spectrum (from 3.1 GHz to 10.6 GHz) for use by UWB devices [10].

The relationship between center frequency and band number is given by the following equation:

$$\text{Band center frequency} = \begin{cases} 2904 + 528 \times n_b & n_b = 1...4 \\ 3168 + 528 \times n_b & n_b = 5...13 \end{cases} \text{(MHz).} \quad (4.6)$$

It provides a numbering system for all channels that have a spacing of 528 MHz within the bands from 3.1 to 10.6 GHz. Bands 1 through 3 are used for Mode 1 devices (mandatory mode), while bands 1 through 3 and 6 through 9 are used for Mode 2 devices (optional mode). The remaining channels are reserved for future use. Table 4.3 summarizes the band allocation.

Table 4.3 OFDM PHY band allocation

BAND_ID	Lower frequency	Center frequency	Upper frequency
1	3168 MHz	3432 MHz	3696 MHz
2	3696 MHz	3960 MHz	4224 MHz
3	4224 MHz	4488 MHz	4752 MHz
4	4752 MHz	5016 MHz	5280 MHz
5	5544 MHz	5808 MHz	6072 MHz
6	6072 MHz	6336 MHz	6600 MHz
7	6600 MHz	6864 MHz	7128 MHz
8	7128 MHz	7392 MHz	7656 MHz
9	7656 MHz	7920 MHz	8184 MHz
10	8184 MHz	8448 MHz	8712 MHz
11	8712 MHz	8976 MHz	9240 MHz
12	9240 MHz	9504 MHz	9768 MHz
13	9768 MHz	10032 MHz	10296 MHz

4.3.2 Channelization

Channelization for different piconet is achieved by using different time-frequency codes for different piconets. In addition, different preamble patterns are used for the different piconets. The time-frequency codes are

defines in Table 4.4 for both Mode 1 (3-band) and Mode 2 (7-band).

For data rates of 55, 80, 110, 160 and 200 Mbps a time-domain spreading operation is performed with a spreading factor of 2. The time-domain spreading operation consists of transmitting the same information over two OFDM symbols. These two OFDM symbols are transmitted over different sub-bands to obtain frequency diversity. For example, if the device uses a time-frequency code [1 2 3 1 2 3], as specified in Table 4.1, the information in the first OFDM symbol is repeated on sub-bands 1 and 2, the information in the second OFDM symbol is repeated on sub-bands 3 and 1, and the information in the third OFDM symbol is repeated on sub-bands 2 and 3.

Table 4.4 Time Frequency Codes and Preamble Patterns for Different Piconets

Channel Number	Preamble Pattern	Mode 1: Length 6 Time Frequency Code						Mode 2: Length 7 Time Frequency Code						
1	1	1	2	3	1	2	3	1	2	3	4	5	6	7
2	2	1	3	2	1	3	2	1	7	6	5	4	3	2
3	3	1	1	2	2	3	3	1	4	7	3	6	2	5
4	4	1	1	3	3	2	2	1	3	5	7	2	4	6

4.4 UWB channel model

Channel models are often derived based on measurements of channel behavior in the environments. The measurements lead to a power delay profile that is a representative of the channel environments.

4.4.1 Measurement of UWB channel environments

All wireless systems must be able to deal with the challenges of operating over a multipath propagation channel, where objects in the environment can cause multiple reflections to arrive at the receiver. All the measurement environments are indoor, as this is the target application for 802.15.3a devices. Different types of indoor environments are analyzed, including residential and office environments. In addition to these environment types, most contributors distinguished between line-of-sight channels and non-line-of-sight channels.

A subset of the measurements are selected for the actual parameterization that leads to a channel model. Part of the measurements is reported in [10].

Since it may be difficult for a single model to reflect all of the possible channel environments and characteristics, the group chose to try and match the following primary characteristics of the multipath channel:

- RMS delay spread

- Power delay profile

- Number of multipath components

4.4.2 The IEEE802.15.3a Standard Model for UWB Communications

The larger bandwidth of UWB channels can give rise to new effects compared to "conventional" wireless channel modeling. For the time-of-arrival statistics, the model uses a Saleh-Valenzuela (S-V) approach [12], as the channel measurements showed multipaths arriving in clusters. This is partly a result of the very fine resolution that ultra-wideband waveforms provide. For example, multipath results from reflections off walls, ceiling, furniture, people, and other objects that may be present within a room. The S-V model is unique in its approach of modeling arrivals in clusters and rays within a cluster. This model distinguishes between "cluster arrival rates" and "ray arrival rates". The first cluster starts by definition at time t = 0, and the rays are arriving with a rate given by a Poisson process with a rate λ.

Mathematically, the impulse response of the multipath model is described as equation (4.7).

$$h_i(t) = X_i \sum_{l=0}^{L} \sum_{k=0}^{K} \alpha_{k,l}^i \delta(t - T_l^i - \tau_{k,l}^i) \qquad (4.7)$$

where,

- $\{\alpha_{k,l}^i\}$ are the multipath gain coefficients, i refers to the impulse response realization, l refers to the cluster, and k refers to the arrival within the cluster,

- $\{T_l^i\}$ is the delay of the lth cluster for the ith channel realization,

- $\{\tau_{k,l}^{i}\}$ is the delay of the kth multipath component relative to the lth cluster arrival time (T_l^i),

- $\{X_i\}$ represents the log-normal shadowing, and i refers to the ith realization,

- T_l = arrival time of the first path of the lth cluster,

- $\tau_{k,l}$ = the delay of the kth path within the lth cluster relative to the first path arrival time, T_l,

- Λ = cluster arrival rate,

- λ = ray arrival rate, i.e., the arrival rate of path within each cluster.

The channel coefficients are defined as a product of small-scale and large-scale fading coefficients, i.e.,

$$\alpha_{k,l} = p_{k,l} \xi_l \beta_{k,l} \qquad (4.8)$$

where,

- $p_{k,l}$ is equiprobable ± 1 to account for signal inversion due to reflections,

- ξ_l reflects the fading associated with the lth cluster,

- $\beta_{k,l}$ is the fading associated with the kth ray of the lth cluster.

The amplitude statistics were found to best fit the log-normal distribution rather than the Rayleigh distribution that was used in the original S-V model.

In order to use the model, several of the above parameters need to be defined, which helps relate the model to actual measurements. Table 4.5 provides some parameters for various line-of-sight and nonline-of-sight (NLOS) channels [12]. Four different measurement environments were defined, namely CM1, CM2, CM3, and CM4. CM1 describes a LOS (line-of-sight) scenario with a separation between transmitter and receiver of less than 4m. CM2 describes a non-LOS situation for the distance between transmitter and receiver of less than 4m. CM3 describes a non-LOS scenario for distances between transmitter and receiver 4-10m. Finally, CM4 describes an environment with strong delay dispersion, resulting in a delay spread of 25ns.

Table 4.5 Multipath channel target characteristics and model parameters

Target Channel Characteristics	CM1	CM2	CM3	CM4
τ_m[ns] (Mean excess delay)	5.05	10.38	14.18	
τ_{rms}[ns] (rms delay spread)	5.28	8.03	14.28	25
NP_{10dB} (number of paths within 10 dB of the strongest path)			35	
NP (85%) (number of paths that capture 85% of channel energy)	24	36.1	61.54	
Model parameters				
Λ[1/nsec] (cluster arrival rate)	0.0233	0.4	0.0667	0.0667
λ [1/nsec] (ray arrival rate)	2.5	0.5	2.1	2.1
Γ(cluster decay factor)	7.1	5.5	14.00	24.00
γ (ray decay factor)	4.3	6.7	7.9	12
σ_1[dB] (standard dev. of cluster lognormal fading term in dB)	3.3941	3.3941	3.3941	3.3941
σ_2[dB] (standard dev. of ray lognormal fading term in dB)	3.3941	3.3941	3.3941	3.3941
σ_x[dB] (standard dev. of lognormal fading term for total multipath realization in dB)	3	3	3	3
Model characteristics				
τ_m	5.0	9.9	15.9	30.1
τ_{rms}	5	8	15	25
NP_{10dB}	12.5	15.3	24.9	41.2
NP (85%)	20.8	33.9	64.7	123.3
Channel energy mean [dB]	-0.4	-0.5	0.0	0.3
Channel energy std dev. [dB]	2.9	3.1	3.1	2.7

4.5 LDPC-based Multi-band OFDM

The Multi-band OFDM system considered in this thesis is based on the IEEE 802.15.3a standard. Figure 4.5 shows the top-level block diagram of the system. It consists of transmitter, IEEE 802.15.3a channel, receiver and BER block which calculates the bit error probability.
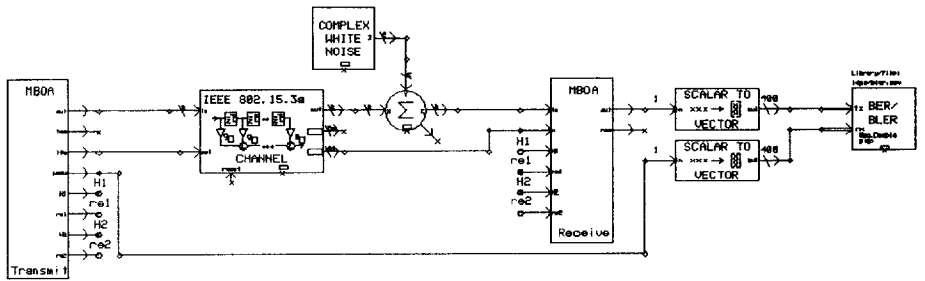

Figure 4.5 Functional block diagram of the simulator

The MB-OFDM transmitter consists of the physical layer convergence procedure (PLCP) frame formatting and data scrambling. The PHY convergence function is supported by the physical layer service data units (PSDU) into a faming format suitable for sending and receiving user data and management information between two or more stations using the associated PMD system [11].

At the first block, the binary information data is coded using a LDPC encoder before being mapped to the QPSK constellation. The dimensions of the LDPC codes are chosen to be identical with the code rates of the IEEE 802.15.3a standard for performance comparison purpose. After using the interleaver, the complex QPSK data pass through a serial-to-parallel

converter and modulated using inverse Fourier Transform (IFFT). **Figure 4.6** shows the bottom level block diagram of the transmitter. Also, LDPC block consists of multiple user-defined blocks.
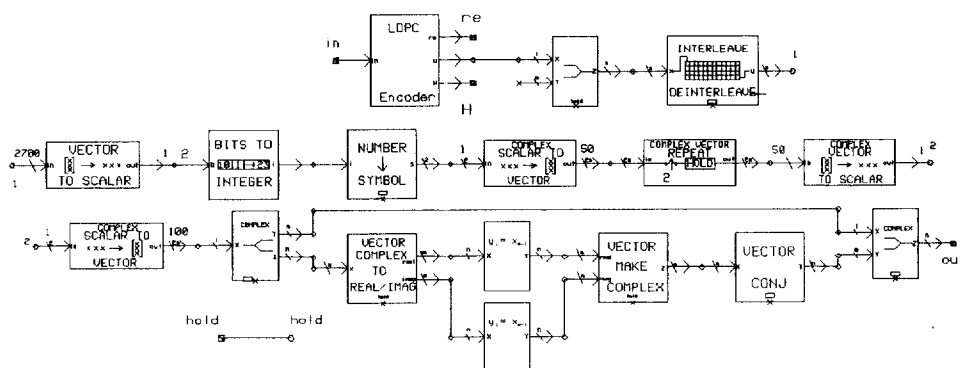

Figure 4.6 Functional block diagram of the MB-OFDM transmitter

A cyclic prefix is appended to the front of baseband signal. The data are spread over both the time and frequency domain. The transmitted signal pass through a frequency selective multipath fading channel model which was proposed by IEEE P802.15 working group 3a for wireless personal area networks with the additive white Gaussian noise (AWGN).

At the receiver, FFT is performed on the received data and then cyclic prefix is removed. The data is converted to by the parallel-to-serial converter before it is decoded using the sum-product algorithm. Figure 4.7 shows the bottom level block diagram of the receiver. The maximum iterations of LDPC decoding is 100.
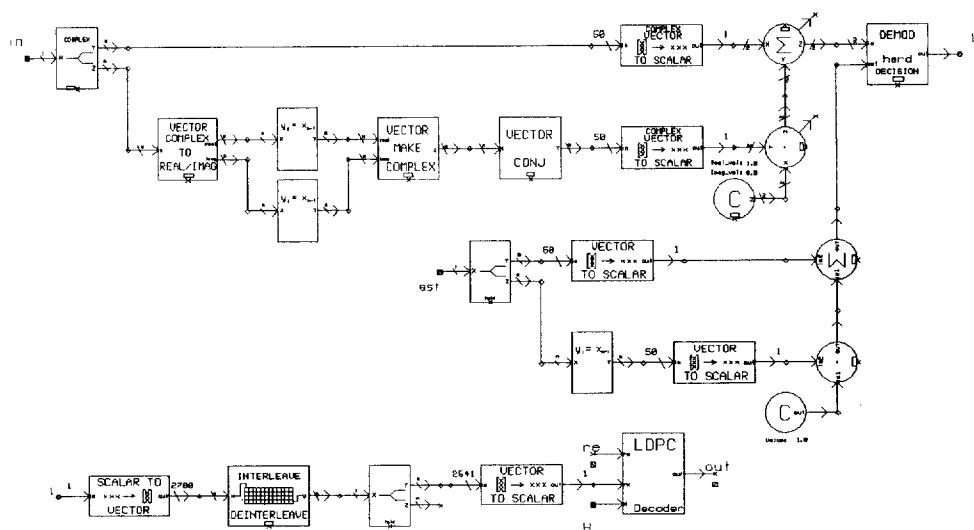
Figure 4.7 Functional block diagram of the MB-OFDM receiver

V. Simulations and discussion

In this thesis, we design and evaluated the performance of Multi-band OFDM system using an irregular LDPC code. In order to investigate the performance of LDPC-based MB-OFDM system, a simulator has been developed using a well-known versatile SPW simulation platform. The simulator consists of a number of SPW standard blocks and user-defined blocks in a hierarchical fashion.

First of all, for the investigation of the performance of LDPC code, the simulation environments are created. We evaluate its performance with the following parameters; BPSK, AWGN, and flat fading. Then, we show the performance of LDPC based Multi-band OFDM system. The channel model 1 (CM1) of the IEEE 802.15.3a is utilized and the channel conditions are assumed to remain unchanged during data symbol duration. Mode 1 operation is considered in the present study, using a time-frequency channelization code [1 2 3 1 2 3] that is set for channel number 1 [2].

5.1 Simulation results of LDPC code

Figure 5.1 shows the BER curves for rate 1/2 of (1008, 504) LDPC code with column weight 3 over the additive white Gaussian noise channel under belief propagation decoding. We can see a similar error performance to the results reported in [13]. The difference between the two results is only 0.06 dB at BER=10^{-3}.
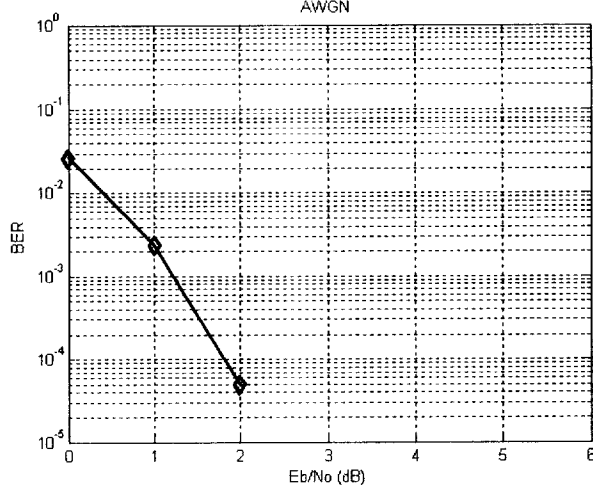
Figure 5.1 BER performance result for AWGN channel

Figure 5.2 shows the BER performance of (1008, 504) LDPC code obtained from the SPW simulation for flat fading model. The maximum iteration is 100 and BPSK modulation is used. The performance of a LDPC code over flat fading environments has not been reported in the literature. For comparison purpose, we instead compare with the performance of the LDPC coded OFDM system over flat fading environments [14]. The comparison reveals that the difference between the two results is 0.02 dB at $BER=10^{-3}$. From these results, it can be said that the performance of the LDPC code is in good agreement with the results previously reported.
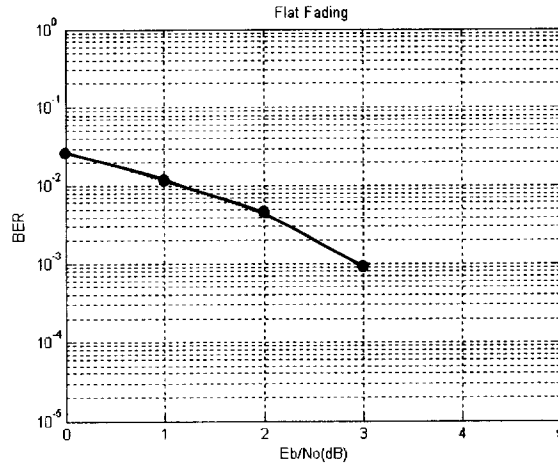
Figure 5.2 BER performance results for flat fading channel

5.2 Simulation results of LDPC based Multi-band OFDM system

Figure 5.3 shows the BER performance of the convolutional encoded system compared with LDPC-encoded system for data transmission speed at 80Mbps. The LDPC-encoded system has a coding gain of 1.21dB at BER of 4×10^{-3} in Channel Model 1. Figure 5.4 represents the result of simulation for the convolutional encoded system and LDPC-encoded system for data transmission speed at 110Mbps. As we see in Figure 5.3 for data rate at 80Mbps, LDPC based system gives better performance in terms of BER. The LDPC-encoded system has a coding gain of 1.32 dB at BER of 4×10^{-3} in Channel Model 1.
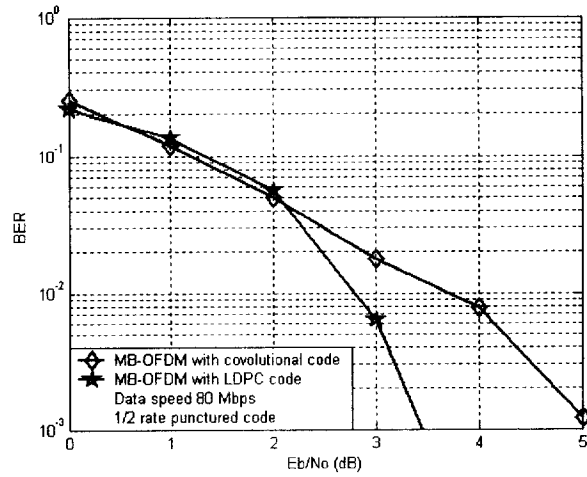
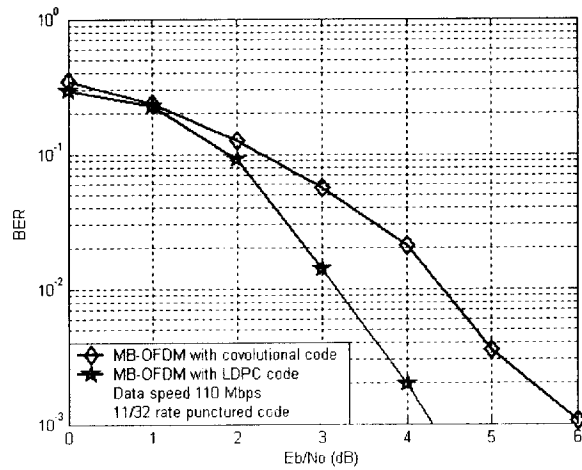Figure 5.3 BER performance for data rate of 80 Mbps

Figure 5.4 BER performance for data rate of 110 Mbps

We also get the similar results in figure 5.5. It shows the BER performance for data transmission speed at 200Mbps. The LDPC-encoded

system has a coding gain of 2.49 dB at BER of 4×10^{-3}. In Figure 5.6, the LDPC code has a coding gain of 3.2 dB at BER of 4×10^{-3} compared with convolutional encoded system.
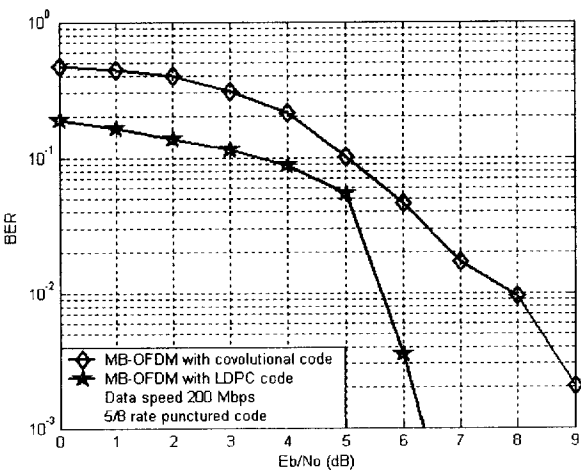

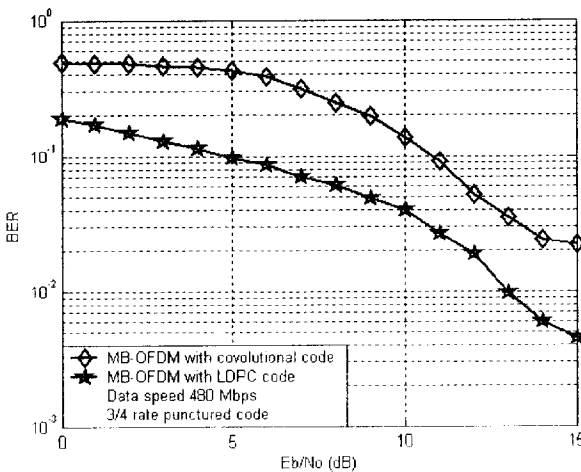Figure 5.5 BER performance for data rate of 200 Mbps

Figure 5.6 BER performance for data rate of 480 Mbps

Figures 5.3-5.6 show the BER performance of the convolutional encoded system compared with LDPC-encoded system for different data transmission speed. Table 5.1 shows the encoding gains at BER of 4×10^{-3} achieved by LDPC over the convolutional codes for similar transmission environment at each data transmission speed. It is also found that the BER performance of the system deteriorates much faster with increasing data transmission speed over the convolutional encoded system compared with the BER performance of the LDPC encoded system. For example, keeping Eb/No fixed at 5dB, the BER at data speed 80 Mbps is 0.0012 and increases to 0.44725 at 480 Mbps for convolutional encoded system, while the BER is 0 for data speed 80 Mbps and increased to 0.09785 for 480 Mbps using LDPC encoded system. The significant performance gain up to 3 dB achieved using LDPC encoding compared to the system presently proposed by the IEEE P802.15 Working Group can significantly improve the quality of service or it can increase the system range for the same power and BER performance.

Table 5.1 Coding gain in dB achieved by LDPC over the convolutional
codes at each data rate

Data Rate (Mbps)	Coding gain in dB at BER of 4×10^{-3}
80	1.21
110	1.32
160	1.39
200	2.49
320	2.8
480	3.2

VI. Conclusions

In this thesis, an MB-OFDM with the LDPC codes applied is proposed. An MB-OFDM system is employed to transmit high speed data in ultra wideband spectrum by dividing the available spectrum into multiple bands. In multicarrier transmission schemes, a powerful error correcting code is applied to enhance the performance. The MB-OFDM system considered in the study is in full conformance with the IEEE 802.15.3a standard. Performance comparison shows that the proposed LDPC-based MB-OFDM provides a significant performance gain over the IEEE 802.15.3a standard. It is found that the LDPC based MB-OFDM offers a significant performance gain up to 3 dB over the IEEE 802.15.3a standard presently proposed by the IEEE P802.15 Working Group. That is, the LDPC code in the MB-OFDM plays an important role in significantly improving the BER performance with little power.

References

[1] D. Porcino and W. Hurt, "Ultra-Wideband Radio Technology: Potential Challenges Ahead", IEEE comm. Mag. Vol. 41, No. 7, pp.64-74, July 2003.

[2] IEEE P802.15 Working Group: "Multi-band OFDM Physical Layer proposal", IEEE P802.15-03/268r2, Nov. 2003.

[3] B. Muquet, Z. Wang, G. B. Ginnakis, M. de Couville and P. Duhamel, "Cyclic prefix or zero padding for wireless multicarrier transmission", IEEE Trans. Comm., Vol. 50, pp.2136-2148, Dec. 2002.

[4] R.G. Gallger, "Low density parity check codes", Cambridge, MA: MIT Press, 1963

[5] D. J. C. Mackay and R. M. Neal, "Near Shannon limit performance of low density parity check codes", Electronics Letters, Vol. 32, No. 18, pp.1645-1646, Aug 1996

[6] M. Ghavami, L.B. Michael, R. Kohno, *Ultra Wideband Signals and Systems in Communication Engineering*, John Wiley & Sons. Ltd., 2004

[7] J. Proakis, Digital Communiatios, 4th ed. New York:McGraw-Hill, 2001.

[8] R. M. Tanner, "A recursive approach to low complexity codes", IEEE Trans. Information Theory, Vol. 27, pp.533-547, Sept. 1981.

[9] D. J. C. Mackay, "Good error-correcting codes based on very sparse matrices", IEEE Trans. Information Theory, Vol. 47, no. 2, pp.399-431, Mar. 1999.

[10] Anuj Batra, Jaiganesh Balakrishnan, G. Roberto Aiello and Jeffrey R. Foerster, "Design of a Multiband OFDM System for Realistic UWB Channel Environments", IEEE transactions on microwave theory and techniques, vol. 52, issue 9, part 1, pp.2123-2138, Sept. 2004.

[11] J. Balakrishana, A. Batra and A. Dabak, "A multi-band OFDM system for UWB communication", Proc. IEEE Ultra Wideband Systems and Technologies Conf., Reston, VA, pp.354-358, Nov. 2003.

[12] A. Saleh and R. Valenzuela, "A statistical Model for Indoor Multipath Propagation", IEEE Journal on Selected Areas in Communications, Vol. SAC-5, No.2, pp.128-137, Feb. 1987.

[13] T. Richardson and R. Urbanke, "The renaissance of Gallager's low-density parity-check codes", IEEE comm. Mag. Vol. 41, Issue 8, pp.126-131, Aug. 2003.

[14] H. Futaki and T. Ohtsuki, "Low-Density Parity-Check (LDPC) coed OFDM Systems with M-PSK", VTC Spring 2002 IEEE, Vol. 2, pp.1035-1039, May, 2002.

감사의 글

앞만 보고 달려온 대학원 2년. 이 시간은 저에게 있어서 가장 큰 발전과 발돋움의 시간이었습니다. 대학원 생활을 보람 있게 보낼 수 있도록 부족한 저를 이끌어주시고 도와주신 모든 분들께 감사의 말씀을 드립니다.

무엇보다도 늘 잘 챙겨주시고 성실, 정직과 학문의 자세에 대한 아낌없는 가르침을 주신 정연호 교수님께 깊은 감사를 드립니다. 논문을 위해 섬세한 지도를 해주신, 늘 따뜻한 웃음으로 반겨주셨던 정신일 교수님, 박규철 교수님께도 감사의 말을 드리고 싶습니다. 저에게는 대학원 생활 그 자체인 소중한 이동전송시스템 연구실. 그 중에서도 학기 초부터 언제나 가까이에서 많은 부분을 같이하고 큰 힘이 되어준 친오빠 같은 완우선배, 항상 격려해주고 인생의 많은 부분에 대해 조언을 해주는 기영선배, 학부시절부터 저에게는 존재만으로도 힘과 용기가 되어준 홍헌선배, 승진선배, 재규선배, 경운선배 언제나 감사합니다. 웃음소리가 예쁜 수연, 속 깊은 수진, 믿음직스러운 동기 병집, 톡톡 튀는 지민, 2년 동안 함께 할 수 있어서 기뻤고 고맙다는 말을 하고 싶습니다.

대학원에서 만난 소중한 인연. 바쁜 와중에도 삶을 돌아볼 수 있는 여유를 알게 해주시는 저에게 있어서 '모리 선생님' 같은 류수아 선배님, 동기 '홍박사' 경동선배. 늘 웃음짓게 하는 후배 정미, 학부시절부터 의지가 되었고 지금까지도 늘 좋은 조언자가 되어주는 명희선배, 언제나 고맙습니다. 또한 변치 않는 우정을 함께 하는 든든한 후원자들(영화, 은경, 지민, 인숙, 주희), 힘들고 지칠 때마다 힘과 용기를 준 사랑하는 친구들(소희, 선아, 민희, 민화, 수진, 미영),

많은 소중한 추억을 안겨준 '마음을 터놓고' 친구들(은정, 연옥, 은지, 소영, 대환, 태우, 경훈, 성엽, 원건, 재민, 수민, 효영)에게도 고마움을 표하고 싶습니다.

마지막으로 행복한 가정의 소중함을 알게 해주신 이 세상 가장 소중하고 존경하는 부모님. 항상 저를 믿어주시고 든든한 버팀목으로 제 편에서 큰 힘이 되어주시는 아버지와 어머니께 마음 깊이 감사 드리고 부족하지만 대학원 생활의 마지막 결실인 이 논문을 바치고 싶습니다.

2006년 2월

류 미 라 드림